Vapor-phase epoxidation of propene over Au/Ti-MCM-41 catalysts: influence of Ti content and Au content

A.K. Sinha [a], S. Seelan [a], T. Akita [a], S. Tsubota [a], and M. Haruta [b,*]

[a] National Research Institute of Advanced Industrial Science and Technology (AIST), Special Division of Green Life Technology, AIST, 1-8-31, Midorigaoka, Ikeda 563-8577, Japan

[b] Research Institute for Green Technology, AIST, Onogawa 16-1, Tsukuba 305-8569, Japan

Received 12 August 2002; accepted 1 November 2002

Ti-MCM-41 samples were used for propene epoxidation using H_2 and O_2 after Au deposition by deposition–precipitation. Au nanoparticles supported on Ti-MCM-41 with Ti incorporated hydrothermally followed by post-synthesis grafting gave higher propene oxide yields than Ti-MCM-41 with Ti incorporated hydrothermally or by grafting. Au L_3-edge EXAFS spectra show the presence of metallic Au for the low Au content (0.21 wt%) catalyst which is more selective to epoxidation, while at high Au loadings (0.42 wt%) oxidic Au species are observed and the catalyst shows lower epoxide selectivity.

KEY WORDS: epoxidation of propene; gold catalyst; Ti-MCM-41; Au/Ti-MCM-41; EXAFS.

1. Introduction

Propene oxide (PO) is an industrially important chemical for the manufacture of polyurethane, unsaturated resins, surfactants and other products. Extensive efforts continue to develop alternative processes for direct gas-phase propene epoxidation using oxygen [1,2] which can replace the currently used environmentally disadvantageous chlorohydrin and hydroperoxide processes [3]. For example, a Pd/TS-1 catalyst for the *in situ* generation of H_2O_2 from H_2 and O_2 has been successfully developed [4,5]. In a series of papers we have reported the vapor-phase epoxidation of propene over highly dispersed nanosize Au particles supported on TiO_2, TiO_2/SiO_2 [6,7] and titanosilicates such as TS-1, TS-2, Ti-β, Ti-MCM-41 and Ti-MCM-48 [8–11]. These findings are now being followed up by other researchers [12,13]. But the problems for industrial viability still exist due to low PO yields and low H_2 efficiency. The efficiency of supported metal catalysts often depends on the metal dispersion and metal–support interaction. The presence of well-dispersed, tetrahedral Ti sites and Au nanoparticles on the support surface is necessary for epoxidation activity [8–13]. It is possible to incorporate titanium into mesoporous MCM-41 supports during hydrothermal synthesis [14,15] or by post-synthesis grafting [16,17].

In the present work, we have studied the influence of Ti incorporation in the mesoporous MCM-41 structure on the vapor-phase propene epoxidation activity using H_2 and O_2 after Au deposition by the deposition–precipitation (DP) method with low Au loading. The nature of the Au species on the Ti-MCM-41 support surface at low and high Au loadings after calcination (at 300 °C) and their influence on epoxidation activity and selectivity is also studied.

2. Experimental

Ti-MCM-41 and MCM-41 supports were hydrothermally crystallized according to literature procedures [10,18]. Ti grafting on the MCM-41 and Ti-MCM-41 support surfaces was performed in an inert atmosphere using titanocene dichloride following the method of Maschemeyer *et al*. [16] and using titanium isopropoxide following the method of Morey *et al*. [17]. The amount of Ti used for incorporation and the amount of Ti in the final MCM-41 support samples are listed in table 1. The catalyst supports prepared by direct hydrothermal Ti incorporation are designated as H(x), those prepared by Ti grafting on titanium-free MCM-41 as G(x), those prepared by hydrothermal Ti incorporation followed by post-synthesis grafting using titanocene dichloride as HG1(x) and those prepared by hydrothermal incorporation followed by post-synthesis Ti grafting using titanium isopropoxide as HG2(x), where x is the mol% of total input Ti during preparation. Au nanoparticles were deposited on the various Ti-containing MCM-41 supports by the DP method [9,10] using aqueous $HAuCl_4$ solution (corresponding to 1–8 wt% Au) and NaOH solution (0.1 N) as precipitant followed by calcination at 300 °C. Catalysts prepared with different Au loadings on H(1.5) support are designated as H(1.5, 2Au), H(1.5, 8Au), etc. All other supports were loaded

* To whom correspondence should be addressed.
E-mail: m.haruta@aist.go.jp

1011-372X/03/0200-0223/0

Table 1
Surface properties of titanium-containing MCM-41 samples

Catalyst (x) [a]	[Ti(h) + Ti(g)] [b]	Ti (mol%) [c]	Surface area [c] ($m^2\,g^{-1}$)	Pore volume [c] ($cm^3\,g^{-1}$)	Au [d] (wt%)	D_{Au} [e] (nm)
H(1.0)	1.0(h)	1.02	1265.1	1.77	0.19	3.1
H(1.5)	1.5(h)	1.49	1270.4	1.80	0.21	2.8
H(3.0)	3.0(h)	2.13	1016.6	0.87	0.29	3.0
HG1(3.0)	1.5(h) + 1.5(g)	2.42	1192.3	1.56	0.32	3.0
HG1(4.5)	1.5(h) + 3.0(g)	3.91	907.3	0.77	0.37	3.3
HG1(5.5)	1.5(h) + 4.0(g)	4.88	882.9	0.72	0.36	3.6
HG2(3.0)	1.5(h) + 1.5(g)	2.51	1029.9	1.09	0.29	3.0
HG2(4.5)	1.5(h) + 3.0(g)	3.66	903.1	0.71	0.33	3.3
HG2(5.5)	1.5(h) + 4.0(g)	4.92	864.9	0.68	0.37	3.8
G(1.0)	1.0(h)	0.93	1223.4	1.71	0.20	3.1
G(1.5)	1.5(g)	1.17	1205.0	1.60	0.22	2.9
G(3.0)	3.0(g)	2.02	906.8	0.52	0.27	3.4

[a] x = mol% of Ti input.
[b] Ti(h), mol% of hydrothermally incorporated Ti; Ti(g), mol% of grafted Ti. Ti incorporation method: samples H(1.0), H(1.5), H(3.0) hydrothermally during synthesis; samples HG1(3.0), HG1(4.5), HG1(5.5) grafting using titanocene dichloride on Ti-MCM-41 (H(1.5)); samples HG2(3.0), HG2(4.5), HG2(5.5) Ti grafting using titanium isopropoxide on Ti-MCM-41 (H(1.5)); samples G(1.0), G(1.5), G(3.0) by Ti grafting on MCM-41.
[c] Before Au deposition.
[d] Actual Au loading measured by ICP (Au content of starting solution was 2 wt%).
[e] A deviation of ±1–3 nm is observed.

with 2 wt% Au in solution and are designated as H(x), G(x), HG1(x) and HG2(x) (where x = mol% Ti).

The actual Au and Ti contents in the catalysts were determined by the inductively coupled plasma (ICP) technique. Transmission electron microscopy (TEM) observations were made using a Hitachi H-9000 instrument to determine the Au particle size and its distribution. X-ray absorption spectra were collected in transmission mode on BL-10B station at the Photon Factory in the National Laboratory for High Energy Physics (KEK, Tsukuba) and EXAFS signals were measured at the Au L_3-edge (11 919 eV). The samples were pretreated in hydrogen and oxygen and then sealed with polyethylene films in nitrogen atmosphere prior to measurements. The k^3-weighted EXAFS function ($\chi(k)k^3$) was Fourier transformed (FT) to obtain radial structure functions.

The catalytic tests were carried out in a vertical quartz reactor (i.d. 10 mm) using a feed containing 10 vol% each of C_3H_6, H_2 and O_2 diluted with Ar passed over the catalyst (0.15 g) bed at a space velocity of $4000\,h^{-1}\,cm^3\,(g.cat)^{-1}$. Prior to testing, the catalysts were first pretreated at 250 °C for 30 min in a stream of 10 vol% H_2 in Ar, followed by 10 vol% O_2 in Ar streams. The feeds and products were analyzed using on-line GCs equipped with TCD (Porapak Q column) and FID (HR-20M column) detectors and auto-injectors. Turn-over frequencies (TOFs) were calculated on the basis of the number of Au particles determined using mean Au particle size and Au weight loadings. A hemispherical Au particle model was assumed and Au metal density of $19.3\,g\,cm^{-3}$ was used.

3. Results and discussion

Table 1 lists the titanium content, BET surface areas and pore volumes of the Ti-containing MCM-41 supports. The actual Au content, actual Ti content obtained by ICP analysis, and Au mean particle size D_{Au} obtained by TEM analysis of Au-loaded catalysts are also listed in table 1. The BET surface areas and pore volumes of the samples were found to decrease with increasing Ti content. Powder X-ray diffraction (XRD) analysis of the various Ti-containing MCM-41 samples showed that all the samples maintain their crystallinity with clear d_{100}, d_{110}, d_{200}, d_{210} diffraction peaks. UV–vis analysis of the Ti-containing MCM-41 samples showed a band near 220 nm which is attributed to tetrahedrally coordinated Ti. With increasing Ti content (from 1.5 to 5.5 mol%) in the samples the UV–vis spectra are found to become broader in the higher wavelength region probably due to formation of Ti–O–Ti-type clusters. The details of the XRD and UV–vis analyses are presented elsewhere [19].

The results of the influence of the mode of Ti incorporation and the amount of Ti incorporated in the MCM-41 support framework on TOF of propene conversion, on TOF of hydrogen conversion and on PO yields for the supported Au catalysts are presented in figure 1. PO is the major reaction product and CO_2 is the main side product. Propanal, ethanal and acetone are very minor side products.

TOF for propene conversion shows an increasing trend with increasing Ti content from 1.0 mol% for catalysts H(1.0) and G(1.0) to 5.5 mol% for catalysts HG1(5.5) and HG2(5.5). However, it has been observed

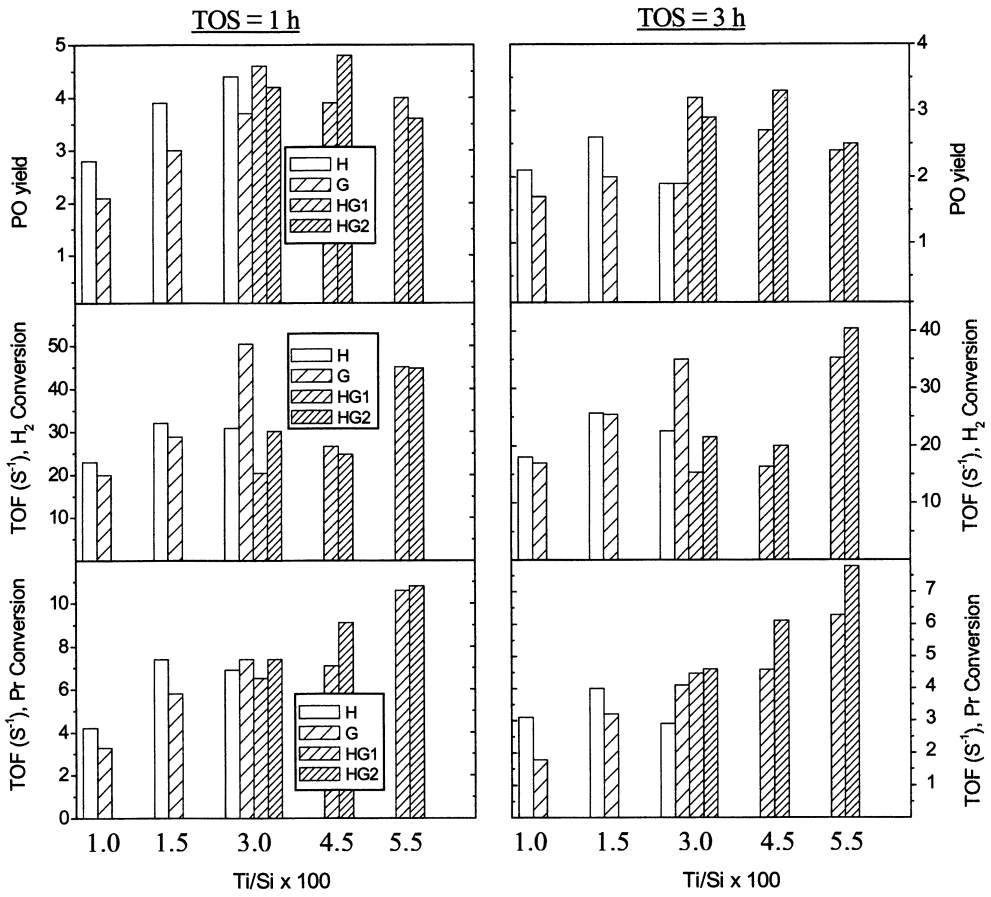

Figure 1. TOF of propene conversion, H_2 conversion and PO yield as a function of Ti content for various Ti-containing MCM-41 samples. H = catalyst with hydrothermally input Ti; G = catalyst with Ti input by grafting; HG1 = catalyst with Ti input hydrothermally followed by grafting using titanocene dichloride; HG2 = catalyst with Ti input hydrothermally followed by grafting using titanium isopropoxide.

previously that for Ti-MCM-41 supports with Ti incorporated hydrothermally, the overall propene conversion of Au catalysts decreases rapidly with increasing amount of Ti beyond 3 mol% Ti content [10]. The catalysts H(1.0) and H(1.5) which contain hydrothermally incorporated Ti show higher TOF for propene conversion than the catalysts G(1.0) and G(1.5) prepared by post-synthesis Ti grafting on MCM-41 surface at low Ti contents (<3 mol% Ti). But the initial TOFs and PO yields are comparable for all the four types of catalysts at 3 mol% Ti content and there is no appreciable increase in the initial PO yield with increasing Ti content (at time on stream (TOS) = 1 h). At very high Ti contents of 5.5 mol% the PO yield decreases even though TOF of propene conversion is highest for these catalysts, which is due to greater CO_2 formation. The catalysts G(x) prepared by Ti grafting on MCM-41 give the lowest PO yields. But for a long time on stream (TOS = 3 h) the catalysts prepared by two-step Ti incorporation (HG1(3.0), HG1(4.5), HG2(3.0) and HG2(4.5)) give higher PO yields than the other type of catalysts, H(x) and G(x). Except for catalyst G(3.0) prepared by 3.0 mol% Ti grafting and catalysts HG1(5.5) and HG2(5.5) prepared by 5.5 mol% Ti incorporation (by two-step method) which show very high TOF for hydrogen conversion, all the other types of catalysts show lower TOF for hydrogen conversion (better hydrogen efficiency).

Our results show that catalysts HG1(x) and HG2(x) with 3.0 and 4.5 mol% Ti incorporated and prepared by the two-step Ti incorporation method deactivate slower than the other catalysts (figure 1). Oligomeric species formed from adsorbed PO on the acidic sites of the catalyst surface via a propoxy species [20] are probably responsible for the deactivation of the Au catalysts supported on titanosilicates like Ti-MCM-41 [10,12,13]. The grafting of Ti occurs at the acidic silanol sites [16] of the MCM-41 surface which probably would reduce the number of silanol groups resulting in less deactivation for the catalyst with Ti grafted on it.

It has been proposed that hydrogen peroxy-like species formed on the Au surface are the oxidant for the epoxidation reaction [8–14] in the reaction temperature range 373–473 K, even though it is still speculative. It would be desirable that Au and Ti sites are in synergism to utilize the *in situ* generated oxidant. The enhanced activity and higher PO yields along with appreciable hydrogen efficiency of the Au catalysts supported on Ti-MCM-41, with up to 4.5 mol% Ti incorporated by the two-step

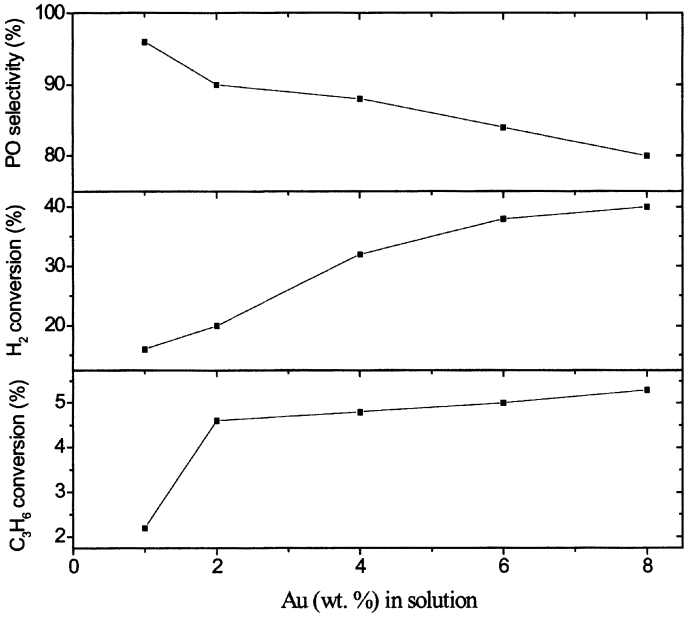

Figure 2. Influence of Au content in solution on propene conversion, hydrogen conversion and PO selectivity of H(1.5) catalyst at 150 °C (space velocity, 4000 h^{-1} cm^3 (g cat)$^{-1}$; catalyst, 0.15 g; feed, $Ar/C_3H_6/H_2/O_2 = 70/10/10/10$; TOS = 1 h).

method, could be attributed to larger concentration of accessible, well-dispersed surface Ti sites which are partly in contact with Au nanoparticles and utilize the *in situ* generated hydroperoxy species for epoxidation more efficiently.

It is observed from figure 2 that with increasing Au content in solution for Au deposition on Ti-MCM-41 sample H(1.5) from 1 to 8 wt% (actual Au loading varies between 0.18 and 0.42 wt%) propene and hydrogen conversions increase whereas PO selectivity is

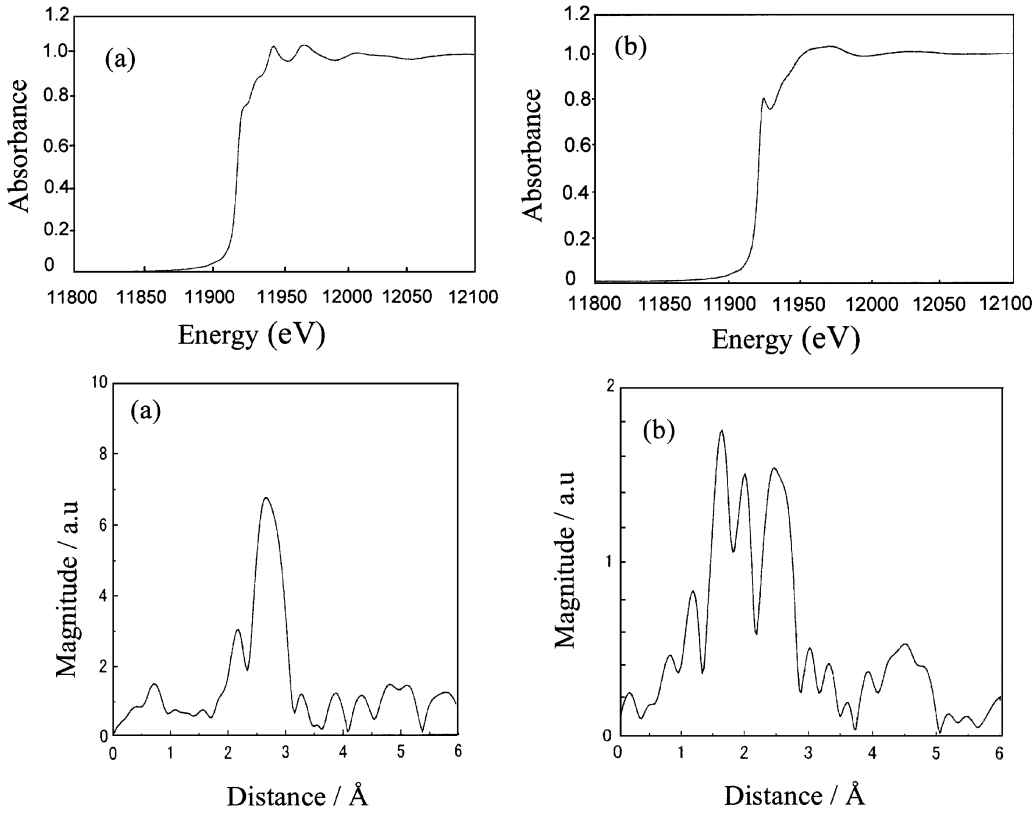

Figure 3. Au L_3 edge EXAFS spectra (top) and Fourier transforms (bottom) of Au k^3-weighted EXAFS of (a) H(1.5, 2Au) with 2 wt% Au loading (actual Au loading 0.21 wt.%) and (b) H(1.5, 8Au) with 8 wt% Au loading (actual Au loading 0.42 wt%).

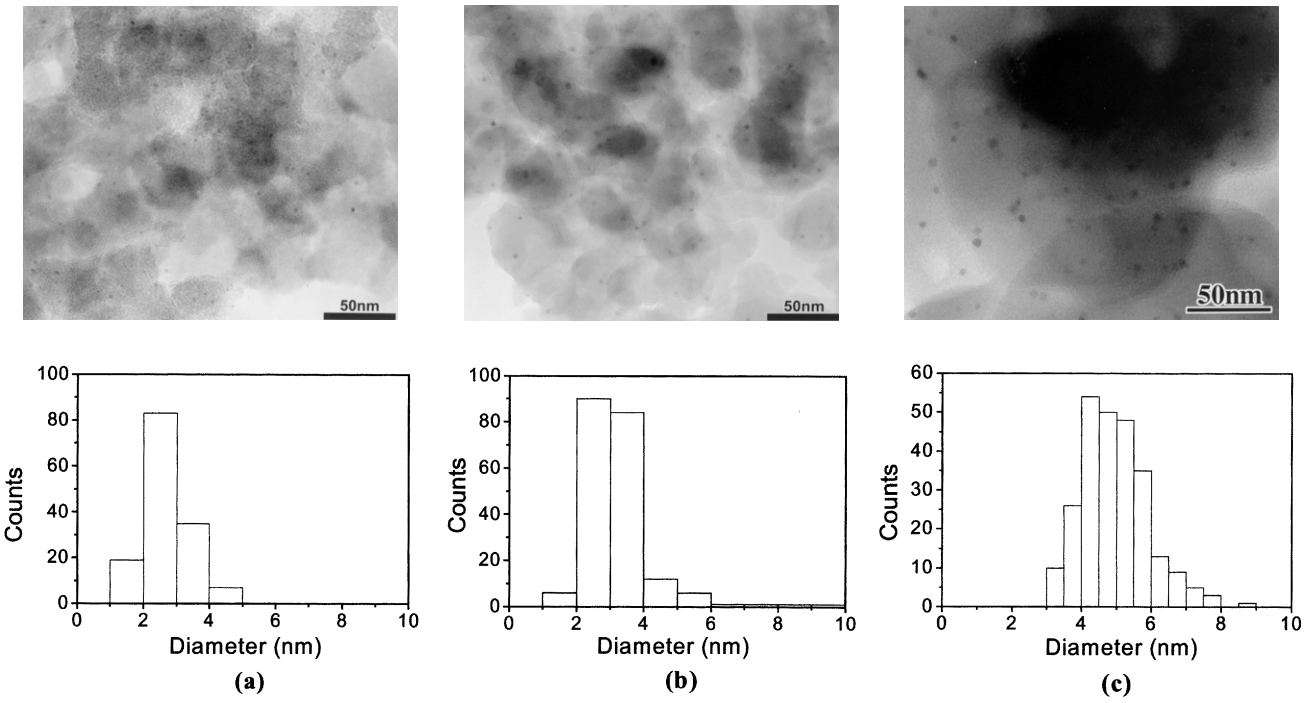

Figure 4. TEM images of Au supported on Ti-incorporated MCM-41 samples and size distribution of Au nanoparticles: (a) H(1.5, 2Au); (b) HG1(5.5); (c) H(1.5, 8Au).

found to decrease due to greater CO_2 formation. The Au L_3 edge normalized XANES spectrum (figure 3(a)) for low Au content (2 wt% Au in solution, actual Au loading, 0.21 wt%) sample H(1.5, 2Au) after calcination at 300 °C is typical of metallic Au [21] and indicates that Au particles are in the metallic state (completely reduced). But the sample H(1.5, 8Au) with high Au content (8 wt% in solution, actual Au loading 0.42 wt%) shows a typical so-called "white line" in the Au L_3 edge normalized XANES spectrum (figure 3(b)). This white line is attributed to an increase in the density of unoccupied *d*-states above the Fermi level of the $2p \rightarrow 5d$ transition [22]. Fourier transforms of the EXAFS spectra also show that the sample with low Au loading, H(1.5, 2Au), shows an intense Au–Au peak due to metallic Au nanoparticles (figure 3(a), bottom) while the sample with high Au loading, H(1.5, 8Au), shows very intense additional peaks (figure 3(b), bottom) due to the presence of Au in higher oxidation states. The magnitude of the Au–Au peaks in the radial distribution function is found to be much lower for the high Au content sample, H(1.5, 8Au), than that for the low Au content sample, H(1.5, 2Au). The sample H(1.5, 8Au) shows a very strong peak at ~1.7 Å due to the presence of an Au–O bond which is indicative of the presence of oxidic Au species in the sample, and another strong peak at around 2.0 Å assigned to Au–M (M = Au, Ti) interaction [23]. However, such peaks are not seen in the Fourier transform of the H(1.5, 2Au) sample. The results suggest that the Au catalysts supported on Ti-MCM-41 are more selective to PO formation when Au is present in the metallic state at lower Au content (catalyst H(1.5, 2Au)) while the high Au content catalyst, H(1.5, 8Au), containing oxidic/unreduced Au species favors total oxidation of propene to CO_2.

Typical TEM images of the Au nanoparticles supported on Ti-MCM-41 samples H(1.5, 2Au), HG1(4.5) and H(1.5, 8Au) and Au particle size distributions are shown in figure 4. Au nanoparticles were found to be uniformly dispersed on the support surfaces. But at higher Au loadings the average particle size is bigger (~5 nm) (figure 4(c)) than that at low Au loadings (particle size ~3 nm) (figure 4(a) and table 1). The presence of larger particles in the high Au content sample is probably responsible for the lower hydrogen efficiency observed over this catalyst due to more H_2O formation. It is also noticed from table 1 and figure 3(b) that at higher Ti contents (5.5 mol%) in the catalysts the average Au particles size increases.

4. Conclusions

Au/Ti-MCM-41 catalysts with up to 4.5 mol% Ti incorporated, partly hydrothermally (1.5 mol% Ti) and partly by grafting using titanium isopropoxide (3.0 mol% Ti), give the highest PO yield and show the lowest TOF for H_2 conversion (best hydrogen efficiency) among all the catalysts studied here with 1.0–5.5 mol% of incorporated Ti. The results indicate that depending on the amount of Ti incorporated by different incorporation methods it is possible to improve the epoxide yield and hydrogen efficiency of the catalyst. Au L_3-edge

EXAFS analysis shows that the nature of the Au species on the support surface after calcination at 300 °C depends on the amount of Au loaded. Low Au loading catalyst (0.21 wt% Au) contains metallic Au particles (with ~3 nm particle size) and the catalyst is more selective to PO. But the high Au loading catalyst (0.42 wt% Au) contains oxidic Au species along with metallic Au particles resulting in lower selectivity to PO (more CO_2 formation) and larger (~5 nm) Au particles for this catalyst, which probably favors undesirable H_2O formation from H_2 and O_2 resulting in lower hydrogen efficiency.

Acknowledgment

A.K. Sinha and S. Seelan gratefully acknowledge the financial support from the Science and Technology Agency of Japan and NEDO, Japan, respectively. We thank Dr. Y. Ichihashi for carrying out the EXAFS measurements.

References

[1] K. Murata and Y. Koyozumi, Chem. Commun. (2001) 1356.
[2] H. Orzesek, R.P. Schulz, U. Dingerdisses and W.E. Maier, Chem. Eng. Technol. 22 (1999) 8.
[3] S.J. Ainsworth, Chem. Eng. News 9 (1992); M. McCoy, Chem. Eng. News 19 (2001).
[4] A. Sato, T. Miyake and T. Saito, Shokubai (Catalysts) 34 (1992) 132.
[5] R. Meiers, U. Dingerdissen and W.F. Hölderich, J. Catal. 176 (1998) 376.
[6] T. Hayashi, K. Tanaka and M. Haruta, Shokubai 37 (1995) 72.
[7] T. Hayashi, K. Tanaka and M. Haruta, J. Catal. 178 (1998) 566.
[8] Y.A. Kalvachev, T. Hayashi, K. Tanaka and M. Haruta, Stud. Surf. Sci. Catal. 110 (1997) 965.
[9] B.S. Uphade, M. Okumura, S. Tsubota and M. Haruta, Appl. Catal. A: Gen. 190 (2000) 43.
[10] B.S. Uphade, Y. Yamada, T. Akita, T. Nakamura and M. Haruta, Appl. Catal. A: Gen. 215 (2001) 137.
[11] C. Qi, T. Akita, M. Okumura and M. Haruta, Appl. Catal. A: Gen. 218 (2000) 81.
[12] T.A. Nijhuis, H. Huizinga, M. Makkee and J.A. Moulijn, Ind. Eng. Chem. Res. 38 (1999) 884.
[13] E.E. Stangland, K.B. Stavens, R.P. Andres and W.N. Delgass, J. Catal. 191 (2000) 332.
[14] A. Corma, M.T. Navarro and J. Perez-Pariente, J. Chem. Soc. Chem. Commun. (1994) 147.
[15] P.T. Tanev, M. Chibwe and T.J. Pinnavaia, Nature 368 (1994) 321.
[16] T. Maschmeyer, F. Ray, G. Sankar and J.M. Thomas, Nature 378 (1995) 159.
[17] M.S. Morey, S. O'Brien, S. Schwarz and G.D. Stucky, Chem. Mater. 12 (2000) 898.
[18] D.W. Hwang, A.K. Sinha, C.-Y. Cheng, T.-Y. Yu and L.P. Hwang, J. Phys. Chem. 105 (2001) 5713.
[19] A.K. Sinha, S. Seelan, T. Akita, S. Tsubota and M. Haruta, Appl. Catal. A: Gen (in press).
[20] G. Mul, A. Zwijnenburg, B. Linden, B. van der, M. Makkee and J.A. Moulijn, J. Catal. 201 (2001) 128.
[21] T.M. Salama, T. Shido, T. Minagawa and M. Ichikawa, J. Catal. 152 (1995) 322.
[22] F.W. Lytle, P.S.P. Wei, R.B. Greegor, G.H. Via and J.H. Sinfelt, J. Chem. Phys. 70 (1979) 4849.
[23] H. Kageyama, S. Tsubota, N. Kamijo and M. Haruta, Jpn. J. Appl. Phys. 32, Suppl. 32-2 (1993) 445.